

# We are IntechOpen, the world's leading publisher of Open Access books Built by scientists, for scientists

6,900

Open access books available

185,000

International authors and editors

200M

Downloads

Our authors are among the

154

Countries delivered to

TOP 1%

most cited scientists

12.2%

Contributors from top 500 universities



WEB OF SCIENCE™

Selection of our books indexed in the Book Citation Index  
in Web of Science™ Core Collection (BKCI)

Interested in publishing with us?  
Contact [book.department@intechopen.com](mailto:book.department@intechopen.com)

Numbers displayed above are based on latest data collected.  
For more information visit [www.intechopen.com](http://www.intechopen.com)



---

# **Boiling of Immiscible Mixtures for Cooling of Electronics**

---

Haruhiko Ohta, Yasuhisa Shinmoto,  
Daisuke Yamamoto and Keisuke Iwata

Additional information is available at the end of the chapter

<http://dx.doi.org/10.5772/62341>

---

## **Abstract**

To satisfy the requirements for the cooling of small and large semiconductors operated at high heat flux density, an innovative cooling method using boiling heat transfer to immiscible liquid mixtures is proposed. Immiscible liquid mixtures discussed here are composed of more-volatile liquid with higher density and less-volatile liquid with lower density, and appropriate volumetric ratios become a key to realize high-performance cooling. The chapter reviews the experimental results obtained by the present authors, where critical heat flux accompanied by the catastrophic surface temperature excursion is increased up to 300 W/cm<sup>2</sup> for FC72/water by using a flat heating surface of 40 mm in diameter facing upwards under the pressure 0.1 MPa.

To apply the superior heat transfer characteristics in boiling of immiscible mixtures to flow boiling system, preliminary experiments using a horizontal heated tube are performed and the classification of flow pattern with liquid-liquid interface and corresponding heat transfer performance are discussed.

**Keywords:** cooling of electronics, immiscible mixture, insoluble mixture, pool boiling, flow boiling

---

## **1. Introduction**

### **1.1. Possibility of non-azeotropic mixtures**

For the systems of air conditioning and refrigeration, non-azeotropic miscible mixtures are often used as the working fluids alternative to the discontinued ones. However, these fluids have a well-known unavoidable disadvantage of heat transfer deterioration resulting from the increased interfacial temperature due to the existence of mass diffusion resistance. At the same

time, for the non-azeotropic miscible mixtures, there is an unknown effect of Marangoni force exerted mainly by the concentration difference along the liquid-vapor interface as a result of the preferential evaporation of more-volatile component. In aqueous solutions of alcohol with a large carbon number, the surface tension is increased with increasing temperature depending on the range of concentration and the level of temperature. In such a condition, Marangoni force due to the concentration gradient is enhanced by also the temperature gradient along the interface, especially near the three-phase interline extended at the base of bubbles. The enhancement of critical heat flux (CHF) was shown by Vochten-Petre [1] and Van Stralen [2] based on the experiments using a wire heater. Abe [3] verified the drastic increase of maximum heat transportation for heat pipes using "self-rewetting mixtures". Sakai et al. [4] confirmed the small enhancement of heat transfer in the ranges of very low alcohol concentration in water, while no appreciable increase in CHF for a flat heating surface facing upwards. As a consequence, non-azeotropic mixtures have no advantage from the view point of the improvement of heat transfer.

## 1.2. Expected performance of immiscible mixtures

Innovative cooling systems which meet the requirement for the increased heat generation density from electronic devices are urgently required. To enhance the values of CHF for the cooling of a large area at high heat flux larger than  $200 \text{ W/cm}^2$  as shown in **Figure 1**, the present authors confirmed the validity of the devised structure which reduces the effective heating length by the liquid supply directly to the downstream of the heating duct from the transverse direction. An example of the structure is illustrated in **Figure 2** [5,6]. However, such structure is rather complicated. On the other hand, to ensure the high reliability for a long-term operation, microstructures on the "enhanced surface" cannot be accepted depending on their application. The present authors noticed the superior heat transfer characteristics in nucleate boiling of immiscible mixtures even on a smooth surface (Kobayashi et al. [7], Ohnishi et al. [8], Kita et al. [9]), which are summarized as follows.

1. The value of critical heat flux is increased by the self-sustained subcooling of less-volatile liquid as a result of the excessive compression by the high partial vapor pressure of more-volatile component.
2. The operation at a pressure higher than the atmospheric is possible keeping low liquid temperature to prevent the mixing of incondensable air which seriously deteriorates the heat transfer in the condensation process, i.e., a final heat dissipation process, due to the existence of mass diffusion resistance.
3. The surface temperature is decreased during the free convection or nucleate boiling of less-volatile liquid, which is caused by the substantial heat transfer enhancement by the existence of vapor bubbles generated from the more-volatile component.
4. The excessive overshooting of the surface temperature at the initiation of boiling can be reduced by the selection of more-volatile component and the optimization of its distribution on the heating surface, which is required, e.g., for the cooling of automobile power controllers with a large fluctuation of thermal load.

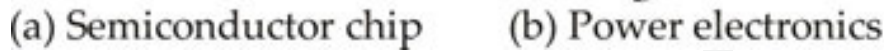


**Figure 1.** Difference in the size and heat flux level of semiconductors as a target of cooling.

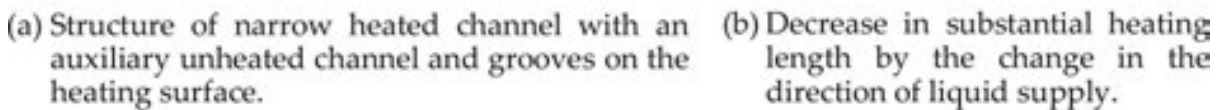


**Figure 2.** Devised structure of cold plate for the cooling by flow boiling in a narrow channel [5,6].

### 1.3. Existing researches on boiling of immiscible mixtures

A large number of reports on nucleate boiling of oil mixtures exist. Filipczak et al. [10] used emulsions of oil and water, where the distribution of two liquids and vapor was investigated at different levels of heat flux. The heat transfer coefficients for high oil concentration were quite smaller than those for pure water, because the free convection of oil dominates the heat transfer to water-oil mixture. At the initial stage of nucleate boiling, foaming was observed before the formation of emulsion. Roesle and Kulacki [11] studied nucleate boiling of FC72/water and pentane/water on a horizontal wire. The discontinuous phase of more-volatile components FC72 and pentane were dispersed in a continuous phase of water, where the concentrations of more-volatile component were varied as 0.2–1.0% and 0.5–2.0%, respectively.

Nucleate boiling of dispersed component or of dispersed and continuous components was observed depending on the level of heat flux. The heat transfer was enhanced by nucleate boiling of dispersed liquid if its volume fraction was larger than 1%. Bulanov and Gasanov [12] studied the heat transfer to four emulsions, n-pentane/glycerin, diethyl ether/water, R113/water and water/oil, where more-volatile liquids were dispersed in the continuous phase of less-volatile liquids. The reduction of surface superheat at the boiling initiation was observed compared to that for pure less-volatile liquids.

On the other hand, the number of investigations on immiscible mixtures which form stratified layers of component liquids before the heating is quite limited. There are old studies by Bonilla and Eisenbuerg [13], Bragg and Westwater [14], Sump and Westwater [15]. Bragg and Westwater [14] classified heat transfer modes for individual layers of liquids. The interpretation of data, however, was not described in detail. Gorenflo et al. [16] studied boiling of water/1-butanol on a horizontal tube, where the liquid mixture becomes soluble or partially soluble depending on its concentration, and levels of temperature and pressure. From the experiments performed under various combinations of concentration and pressure, they reported that the nucleate boiling heat transfer is not largely depending on the solubility.

## 2. Immiscible mixtures

### 2.1. Phase equilibrium

Immiscible mixtures employed here consist of insoluble component liquids and their phenomena during nucleate boiling have a unique feature characterized by self-sustaining subcooling of liquids. An example of phase equilibrium diagrams for FC72/water at the total pressure of 0.1 MPa is shown in **Figure 3**. The concentration where the two curves merge, which is corresponding to the azeotropic point frequently observed in miscible mixtures, is the concentration of vapor phase independent of the liquid composition for immiscible mixtures. The concentrations  $Y_1$  and  $1-Y_1$  ( $=Y_2$ ) on the dew point curves for lower and higher concentrations of more-volatile component in liquid phase are calculated by the following equations, respectively (e.g., Prigogine and Defay [17]).

$$\ln Y_1 = -\frac{h_{fg,1}}{R_1} \left( \frac{1}{T} - \frac{1}{T_{sat,1}} \right) \quad (1)$$

$$\ln(1 - Y_1) = -\frac{h_{fg,2}}{R_2} \left( \frac{1}{T} - \frac{1}{T_{sat,2}} \right) \quad (2)$$

where  $Y_1$ : mole fraction of more-volatile component in vapor on dew point curve [–],  $T$ : dew point temperature [K],  $T_{sat}$ : saturation temperature [K] for a given total pressure,  $h_{fg}$ : latent heat of vaporization [kJ/kg] and  $R$ : gas constant [kJ/kg·K]. The equations are easily derived from

the Clausius-Clapeyron equation and the ideal gas relation applied approximately to vapor phase.

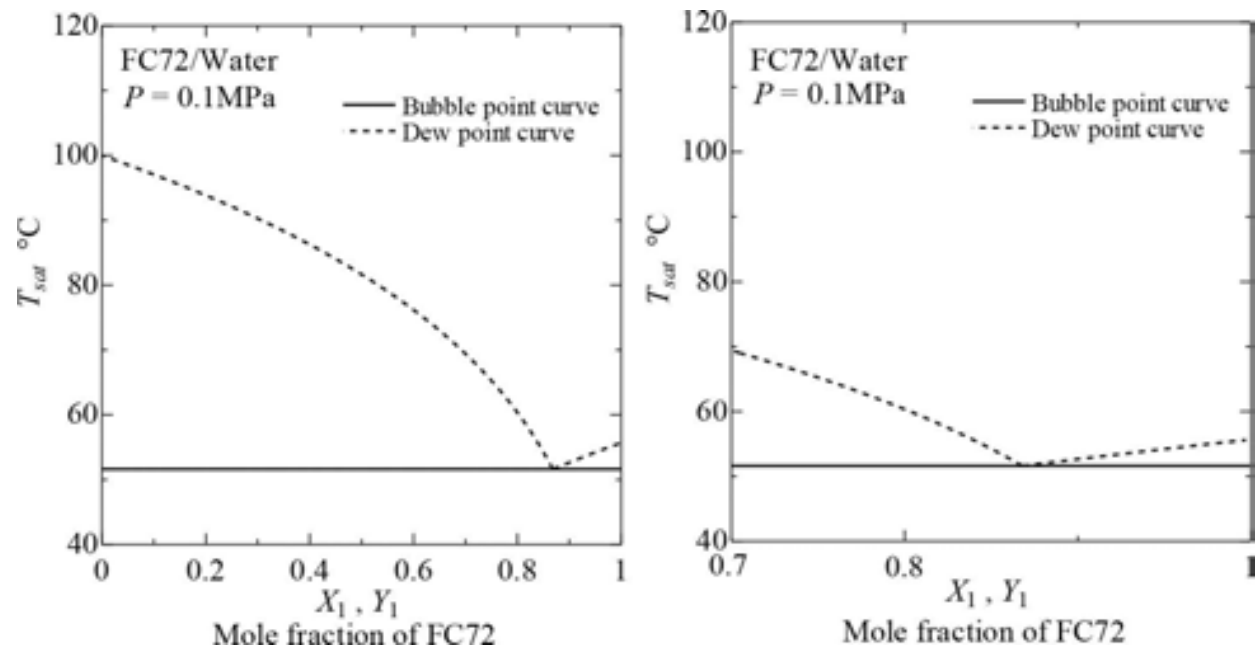


**Figure 3.** Phase equilibrium diagram of FC72/water mixture.

## 2.2. Conditions of component liquids

The conditions of liquid phase are represented in **Figure 4**, where two saturated vapor pressure curves with a red line for a more-volatile component and a blue line for a less-volatile one are drawn. Since immiscible mixtures have the total pressure  $P_{total}$  as the sum of saturated vapor pressures corresponding to the equilibrium temperature  $T_e$ , the equilibrium state of the mixture is represented by a black point in the figure and the relation  $P_{sat,1}(T_e) + P_{sat,2}(T_e) = P_{total}$  holds true. Immiscible liquids are separated because of the difference in their densities, and one component liquid contacts or tends to contact the surface located at the bottom. The equilibrium temperature of immiscible mixtures is realized by the evaporation of both components. The degree of subcooling becomes the difference between the saturation temperature of each component corresponding to the total pressure and the equilibrium temperature of the mixture. If either of two components is not evaporated enough or not satisfy the saturation state corresponding to the equilibrium temperature but the vapor of one component is superheated, the liquid state of the other component is deviated from the equilibrium state represented in the figure. The equilibrium temperature of mixtures tested here and the degree of subcooling for each component liquid are shown in **Tables 1** and **2**, respectively. The subcooling of less-volatile liquid excessively compressed by the high vapor pressure of more-volatile component becomes very high, while the subcooling of more-volatile liquid is very low.



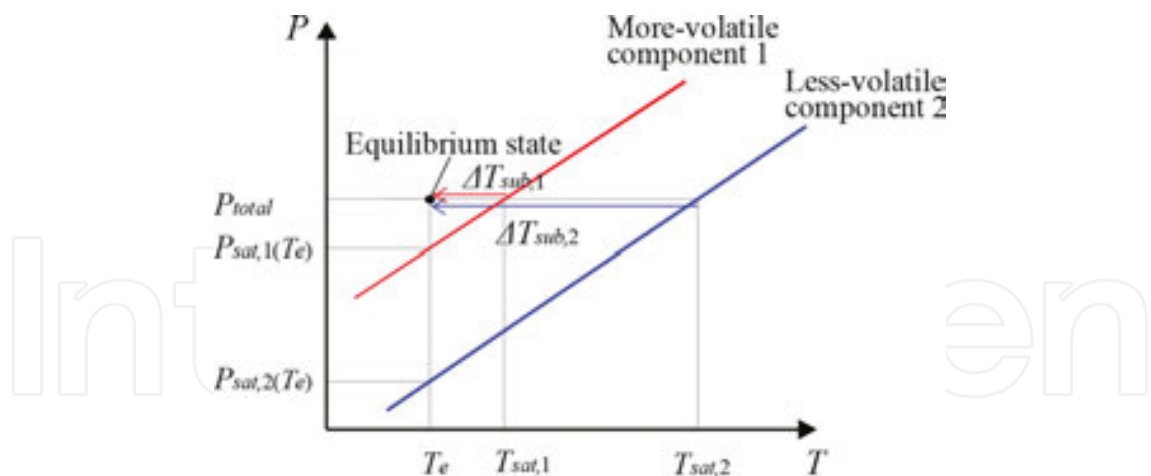


Figure 4. Vapor pressure curves of components for immiscible mixtures.

| More-volatile component ( $T_{sat,1}$ ) | Less-volatile component ( $T_{sat,2}$ ) | Mixtures<br>$T_e$ |
|---|---|-------------------|
| FC72 (55.9°C)                           | Water (100°C)                           | 51.6°C            |
| Novec7200 (78.4°C)                      | Water (100°C)                           | 66.4°C            |

Table 1. Saturation temperature of each component and equilibrium temperature of immiscible mixtures at 0.1 MPa

| Mixtures        | Subcooling                                 |  |
|-----------------|--|--|
|                 | More-volatile component $\Delta T_{sub,1}$ | Less-volatile component $\Delta T_{sub,2}$ |
| FC72/Water      | 4.3 K                                      | 48.4 K                                     |
| Novec7200/Water | 12.0 K                                     | 33.6 K                                     |

Table 2 Degree of subcooling for component liquids at 0.1 MPa

### 3. Pool Boiling

#### 3.1. Experimental apparatus for pool boiling

The outline of the apparatus is shown in **Figure 5**. A flat heating surface of 40 mm in diameter made of copper is located horizontally facing upwards. The upper surface of cylindrical copper heating block is operated as the heating surface surrounded by a thin fin cut out in one unit body to prevent the preferential nucleation at the periphery. Nineteen cartridge heaters are inserted in the heating block and the maximum amount of heat generation is 5700 W. Eight thermocouples are inserted in the center and side of copper heating block at four different depths of 1, 7, 13 and 19 mm below the heating surface to estimate the heat flux and heating surface temperature. Fluid temperatures are measured by three thermocouples at 2, 80 and

160 mm above the heating surface in the boiling vessel, where the liquid level is located between the second and third thermocouples.

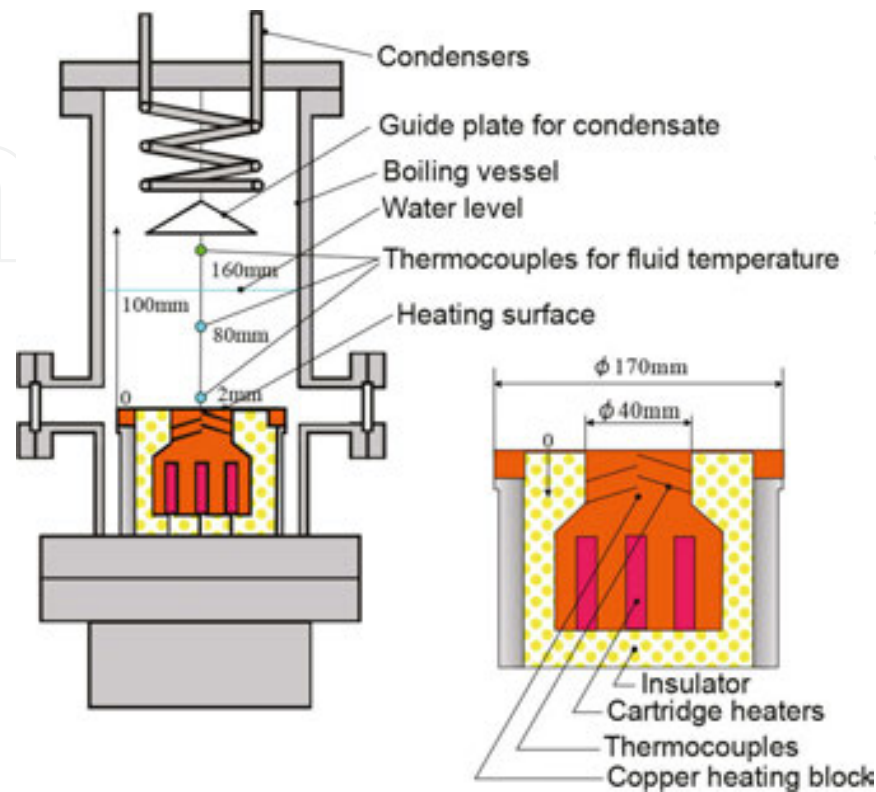


**Figure 5.** Outline of pool boiling experimental apparatus.

The experiments are performed at 0.1 MPa changing volume ratio of the components. Immiscible mixtures of FC72/water and Novec7200/water are used as test fluids, where FC72 and Novec7200 are more-volatile components with higher density and water is less-volatile one with lower density. The conditions for the volume ratio of component liquids are represented by **Figure 6** [9], where  $H_1$  is the height of the more-volatile liquid from the heating surface and  $H_2$  is for the less-volatile liquid. The total height is kept at 100 mm, i.e.,  $H_1 + H_2 = 100\text{mm}$ , and tested compositions are listed in **Table 3**.

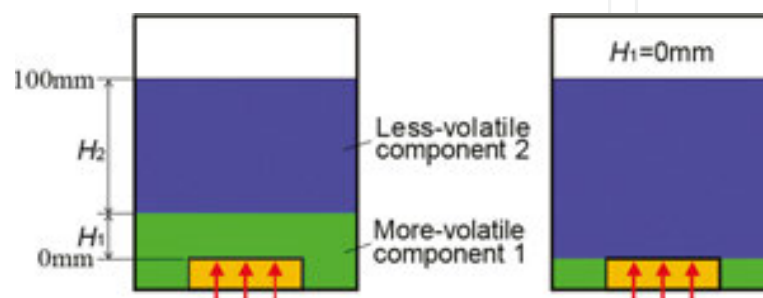


**Figure 6.** Condition representing volume ratio of immiscible liquids [9].



| 1. More-volatile c. / 2. Less-volatile c. | Height of liquid<br>[ $H_1$ mm / $H_2$ mm] |
|---|--|
| FC72/Water                                | [0/100], [5/95], [10/90], [50/50]          |
| Novec7200/Water                           | [0/100], [5/95], [10/90]                   |

Table 3. Tested composition of liquids

3.2. Experimental results for pool boiling

Experimental results are shown in **Figures 7 and 8** for FC72/water and Novec7200/water, respectively. **Figure 7** represents the relation between heat flux  $q$  and heating surface temperature  $T_w$  for FC72/water, where representative heat transfer characteristics of immiscible liquids are known. Independent of volume ratios, the heating surface temperatures for mixtures are located between those for pure liquids. The curve for [50 mm/50 mm] almost coincides with that for the saturated boiling of FC72. For [10 mm/90 mm], a temperature jump similar to burnout phenomena occurs, which is referred to as the "intermediate heat flux burnout" by the present authors. For [5 mm/95 mm] and [0 mm/100 mm], the surface temperature increases with heat flux, where the heat transfer mode changes from natural convection to nucleate boiling of water under high subcooled conditions. For [5 mm/95 mm], the reduction of surface temperature from that of saturated nucleate boiling of water is clearly observed at high heat flux due to the heat transfer enhancement resulting from the generation of bubbles composed mainly by FC72 vapor. For [0 mm/100 mm], the value of CHF increases from 1.35 MW/m<sup>2</sup> of saturated water to 3.04 MW/m<sup>2</sup> of FC72/water mixtures at 0.1 MPa. The marked increase of CHF resulted from the high subcooling of water as much as 48.4 K due to the excessive compression by FC72 vapor. Similar results are obtained also for Novec7200/water despite of the quantitative difference in the effect of liquid height between the two mixtures tested here. In **Figure 9**, the values of CHF are compared with those of subcooled boiling of

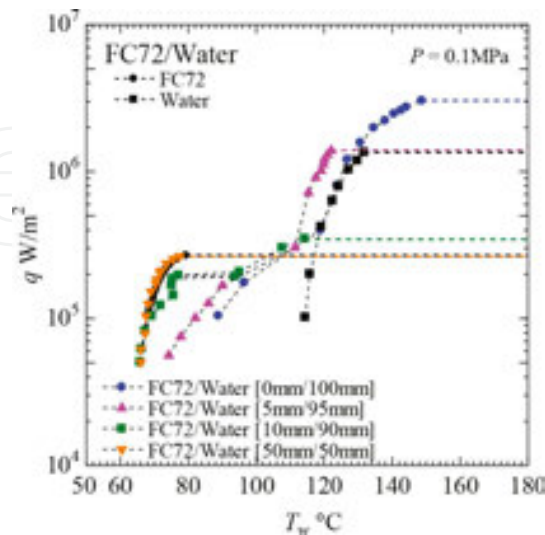


Figure 7. Heat flux versus heating surface temperature for FC72/water.

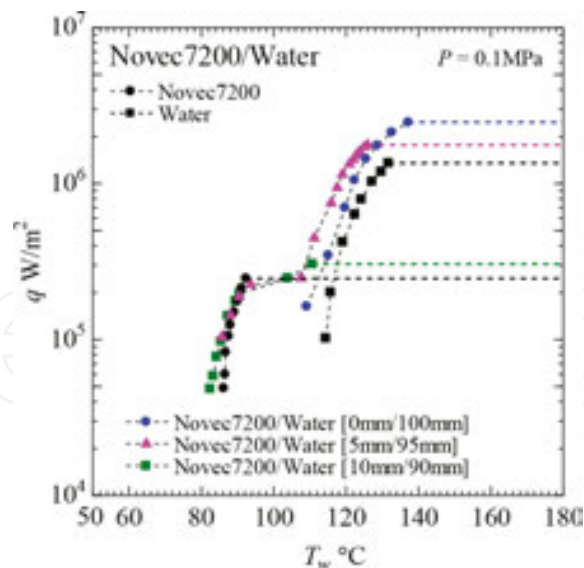


Figure 8. Heat flux versus heating surface temperature for Novec7200/water.

pure water estimated by Ivey-Morris correlation [18]. For [0 mm/100 mm], the experimental CHF values are close to the predicted ones, while the discrepancy is increased as the liquid height of more-volatile component increases. This is because boiling of the more-volatile component promotes the coalescence of bubbles and the dryout occurs at lower heat fluxes.

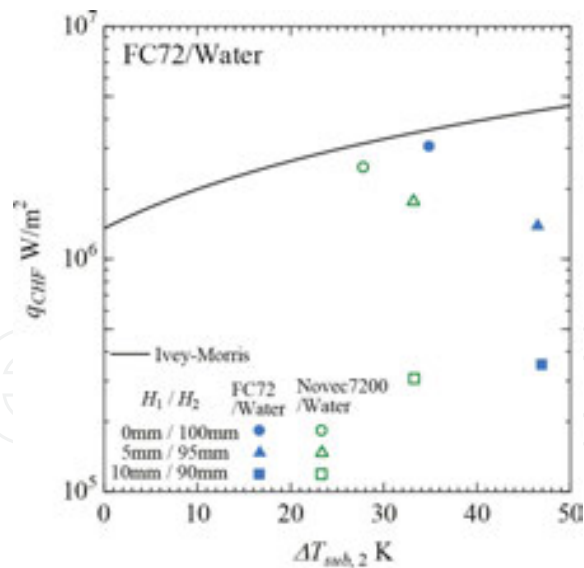


Figure 9. The comparison of CHF data with predicted values for subcooled boiling of less-volatile liquid.

### 3.3. Consideration on the mechanisms of intermediate heat flux burnout

The phenomena of limited jump of heating surface temperature referred here to as the intermediate heat flux burnout occurs if the thickness of the more-volatile liquid with higher

density attached to the horizontal heating surface is small as observed for FC72/water [10 mm/90 mm] at  $q = 2.0 \times 10^5 \text{ W/m}^2$  in **Figure 7** and Novec7200/water [5 mm/95 mm] at  $q = 2.3 \times 10^5 \text{ W/m}^2$  in **Figure 8**.

After the jump of the surface temperature, the heat transfer mode is changed from the nucleate boiling of more-volatile liquid to the natural convection or nucleate boiling of less-volatile liquid at higher heat fluxes. It is very important that the generation of bubbles or vapor slugs of more-volatile component continues also in this region enhancing the heat transfer to the less-volatile liquid. The intermediate heat flux burnout is observed when Taylor instability occurs by the growth of a coalesced bubble with more-volatile component after its lateral coalescence below the bulk of less-volatile liquid with lower density.

The value of minimum bubble diameter  $d_{min}$  penetrating across the liquid-liquid interface is evaluated from the minimum volume of a bubble  $V_{min}$ , assuming the sphere bubble shape (Greene et al. [19], Onishi et al. [20]).

$$V_{min} = \left[ \frac{3.9\sigma}{g(\rho_{L2} - \rho_{V1})} \right]^{\frac{3}{2}} \quad (3)$$

where  $\sigma$ : interfacial tension [m/s],  $g$ : gravitational acceleration [ $\text{m/s}^2$ ],  $\rho_{L2}$ : density of upper liquid, i.e., less-volatile liquid with lower density [ $\text{kg/m}^3$ ],  $\rho_{V1}$ : density of lower vapor, i.e., vapor mainly of more-volatile component [ $\text{kg/m}^3$ ]. The correlation implies that the penetration criteria is determined by two conflicting forces of the buoyancy acting upwards on a bubble and of the interfacial tension to suppress the bubble penetration. **Table 4** listed the most dangerous wavelength of Taylor instability  $\lambda_d$ , minimum bubble penetration diameter  $d_{min}$  and bubble departure diameter  $d_b$  under pool boiling conditions evaluated at 0.1 MPa.

| More-volatile component                     | FC72  | Novec7200 |
|---|-------|-----------|
| Less-volatile component                     | Water | Water     |
| Most dangerous wavelength $\lambda_d$ [mm]  | 28.9  | 28.4      |
| Minimum penetration diameter $d_{min}$ [mm] | 4.2   | 3.9       |
| Bubble departure diameter $d_b$ [mm]        | 0.36  | 0.43      |

**Table 4.** Wavelength for Taylor instability and minimum bubble diameter for more-volatile component to penetrate into upper less-volatile liquid at 0.1 MPa

Bubbles of more-volatile component grow by the evaporation or lateral coalescence in the vicinity of liquid-liquid interface and become sizes beyond  $d_{min}$ . The enlarged bubbles penetrate into the less-volatile liquid layer accompanying the entrainment of more-volatile liquid as shown in **Figure 10**. Under this condition, bubbles of more-volatile component do not grow to the size of the wavelength  $\lambda_d$ , and no mixing of liquids occurs in the vicinity of heating surface. The penetration of generated bubbles thorough the liquid-liquid interface delays their

coalescence. However, at a certain value of heat flux, the rate of bubble generation exceeds the elimination of bubbles by the penetration, and the lateral bubble coalescence occurs under the liquid-liquid interface. The diameter of flattened bubble radius exceeds the wave length of Taylor instability  $\lambda_d$ , and the less-volatile liquid descends and starts to contact the heating surface. The large subcooling of less-volatile liquid is enough to suppress the excessive jump of heating surface temperature.

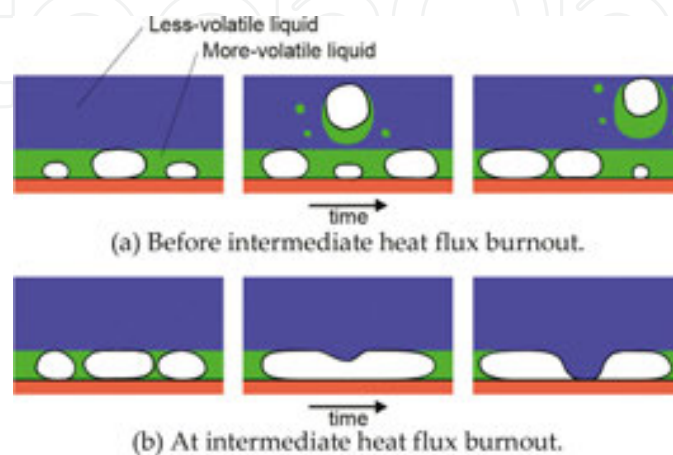


**Figure 10.** Expected behaviors of bubble in the vicinity of liquid-liquid interface.

There is another type of intermediate heat flux burnout confirmed by the present authors, where the heating surface temperature gradually deviates from that for nucleate boiling of pure more-volatile liquid [9]. In such a case, bubbles can coalesce easily below the liquid-liquid interface because of thicker thickness of its layer and exceed the value of most dangerous wave length at lower heat flux. As a consequence, the less-volatile liquid starts to contact partially the heating surface, and the contribution of the heat transfer to the less-volatile liquid gradually increased as the increase of heat flux keeping the steady-state conditions at each heat flux level. Similar phenomenon occurs in the cases of smaller wavelength of Taylor instability or of partially soluble combination of liquids depending on the selection of component liquids. It is clear that the physical and/or chemical mixing of component liquids is a key factor to determine the heat transfer characteristics at low heat flux.

## 4. Flow boiling

### 4.1. Experimental apparatus for flow boiling

**Figures 11 and 12** show the outline of test section and test loop [21]. Test loop is composed of test section, condenser, liquid-vapor separation tank, circulating pump, pre-heater. Immiscible liquids are stratified in liquid-vapor separation tank, and both flow rates are controlled by valves. The test section is composed of a heated section of stainless tube spirally coiled by sheath heaters on the outer surface and a transparent unheated section of Pyrex glass for the observation of liquid-liquid and liquid-vapor interfaces. The inner diameter of both tubes is 7

mm and heated length is 310 mm. Six thermocouples are inserted in the top and bottom tube walls at the upstream, midstream and downstream locations. The experiments are conducted for the combination of FC72 and water, i.e. more-volatile component with higher density and less-volatile one with lower density whose saturation temperatures as pure components are 55.7 and 100°C, respectively, at 0.1 MPa.

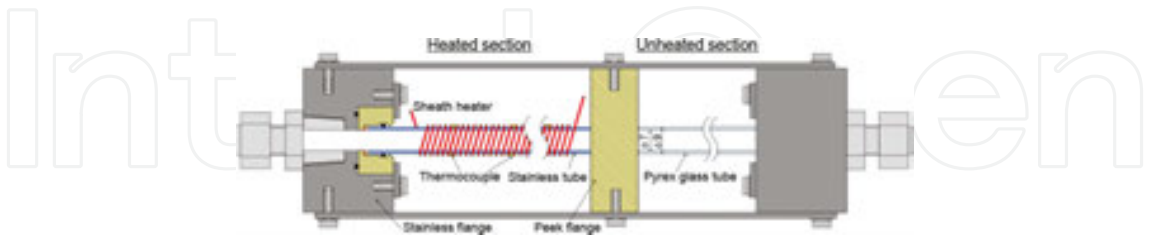


Figure 11. Outline of test section [21].

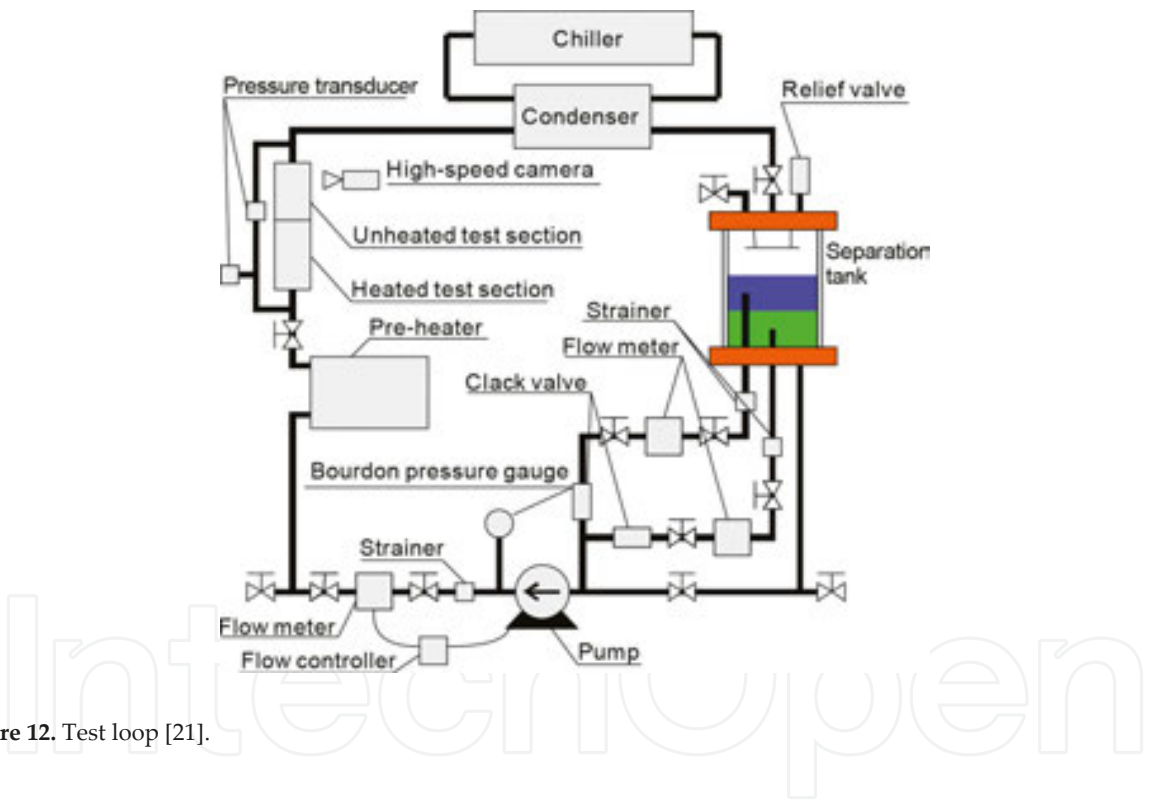


Figure 12. Test loop [21].

4.2. Experimental results for flow boiling

Various flow patterns such as stratified flow, FC72 slug flow, emulsion-like flow, "wavy stratified + FC72 droplet flow", "FC72 churn + FC72 droplet flow" and "FC72 slug + FC72 droplet flow" are observed depending on the combinations of flow rates for both components under unheated conditions, and they are summarized as a liquid-liquid flow pattern map in **Figures 13 and 14** [21]. It is known by the preliminary experiments that the heat transfer characteristics at low heat fluxes are strongly influenced by the liquid-liquid behaviors under unheated conditions.

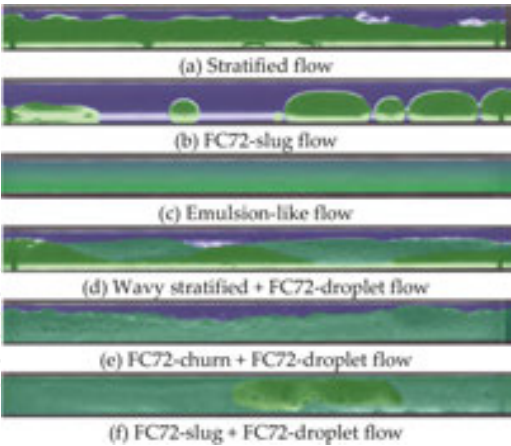


Figure 13. Typical flow patterns of FC72/water [21].

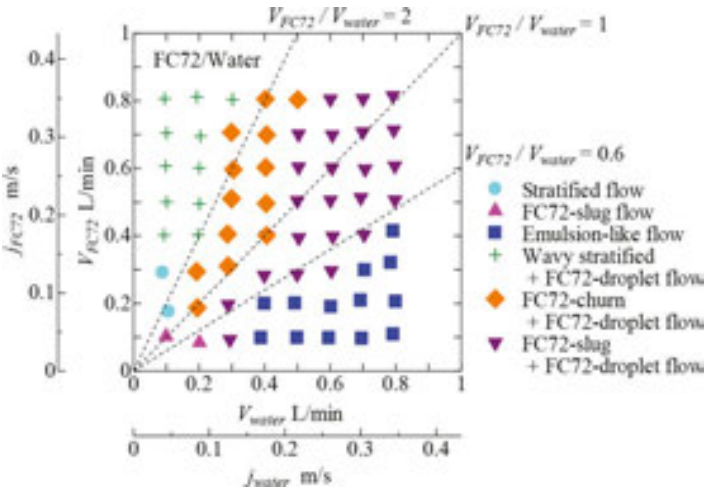


Figure 14. Flow pattern map for FC72/water. [21]

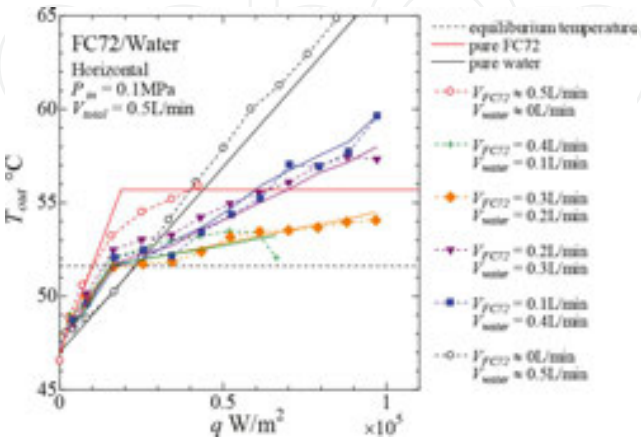


Figure 15. Outlet fluid temperature versus heat flux.



: Water,  : FC72,  : Emulsion



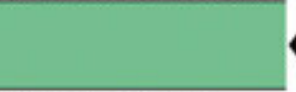






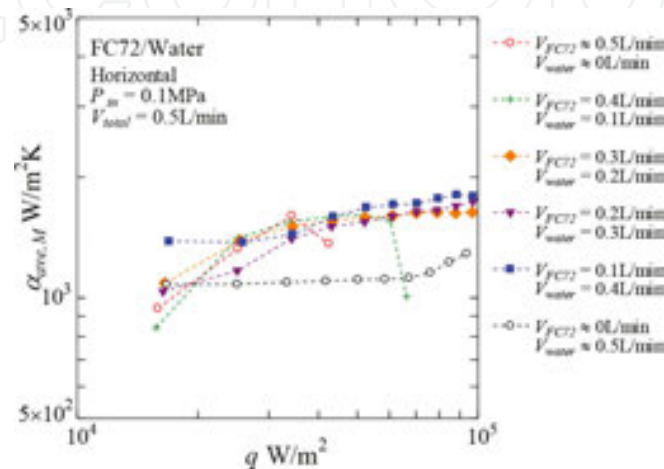
|                    | Stratified flow  | FC72 slug flow  | Emulsion flow   |
|--------------------|--|---|---|
| Very low heat flux | Top: Forced convection of water<br><br>Bottom: Forced convection of FC72  | Top: Forced convection of water<br><br>Bottom: Forced convection of FC72 and water   | Top: Forced convection of water and FC72 emulsion<br> ← Flow<br>Bottom: Forced convection of water and FC72 emulsion   |
| Low heat flux      | Top: Forced convection of water with increased velocity by generation of FC72 bubbles<br><br>Bottom: Nucleate boiling of FC72 | Top: Forced convection of water with increase velocity by generation of FC72 bubbles<br><br>Bottom: Nucleate boiling of FC72 | Top: Two-phase forced convection due to boiling of FC72 and convection of water and FC72 emulsion<br> ← Flow<br>Bottom: Two-phase forced convection due to boiling of FC72 and convection of water and FC72 emulsion   |
| Moderate heat flux | Top: Forced convection by FC72 vapor<br><br>Bottom: Nucleate boiling of FC72  | Top: Forced convection by FC72 vapor + Water liquid phase flow boiling<br><br>Bottom: Nucleate boiling of FC72             | Top: Two-phase forced convection due to boiling of FC72 and convection of water and FC72 emulsion<br> ← Flow<br>Bottom: Two-phase forced convection due to boiling of FC72 and convection of water and FC72 emulsion |

Table 5. Liquid-vapor behaviors for flow boiling of FC72/Water

To evaluate the local heat transfer coefficients, the distribution of mixture temperature along the tube axis is needed. Outlet mixture temperature can be reproduced by the heat balance equations which introduce a parameter  $\xi$  representing the ratio of heat supplied to more-volatile component FC72 to the total. **Figure 15** shows the outlet mixture temperature versus heat flux. The solid lines and broken lines are calculated and experimental outlet temperatures,

respectively. The parameter  $\xi$  depends only on the flow rate ratio and not on the heat flux. This could be possible if the liquid-liquid flow pattern is not strongly dependent on the bubble generation at low heat flux as shown in **Table 5**. The error of the prediction is less than  $\pm 1.0\text{K}$ .

**Figures 16 and 17** show heat transfer coefficient and wall temperature versus heat flux at midstream averaged by the top and the bottom values. Heat transfer coefficient is higher and wall temperature is lower than pure water for immiscible liquid because the convection of water is enhanced by the generation of FC72 bubbles.



**Figure 16.** Heat transfer coefficient versus heat flux at midstream.

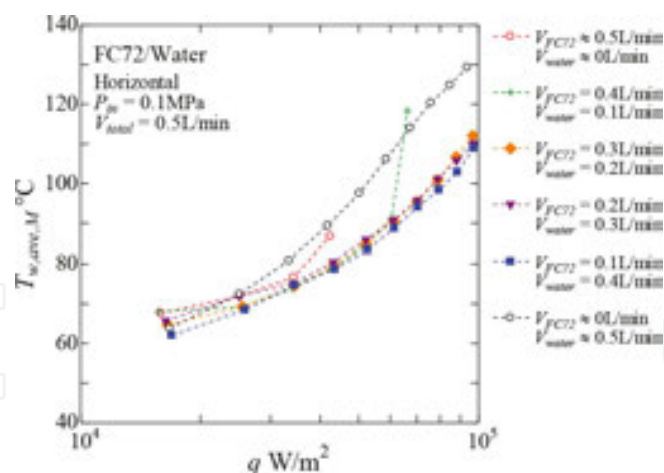


**Figure 17.** Wall temperature versus heat flux at midstream.

## 5. Conclusions

To clarify the boiling heat transfer characteristics of immiscible mixtures, experiments of pool boiling and flow boiling in a tube were conducted, and the following results were obtained.

1. By optimizing the volume ratio of immiscible mixtures in pool boiling using a flat heating surface facing upwards, the drastic increase of CHF and/or the decrease of heating surface temperature from those of pure less-volatile component become possible.
2. The above characteristics resulted from the self-sustaining high subcooling of less-volatile liquid and the substantial heat transfer enhancement caused by the preferential evaporation of more-volatile liquid.
3. In flow boiling, outlet fluid temperature is well reproduced by heat balance equations, which introduced a parameter representing the ratio of heat supplied to more-volatile component to the total.
4. In flow boiling, at low and moderate heat fluxes, the convection of less-volatile liquid is enhanced by boiling of more-volatile liquid, and the enhancement is largest corresponding to the flow pattern of emulsion-like flow at low flow rate of more-volatile component classified under the unheated conditions.

For the cooling systems in an enclosure, the distribution of liquid layers for both immiscible components becomes a key to determine the heat transfer characteristics due to nucleate boiling. For a vertical heating surface or a heating surface operated under the reduced gravity conditions, some methods to transfer the heat to the more-volatile liquid with larger density are needed to obtain the superior cooling characteristics.

## 6. Nomenclature

|             |  |
|-------------|--|
| $h_{fg}$    | latent heat of vaporization, J/kg          |
| $H$         | height of liquid, mm                       |
| $j$         | superficial velocity, m/s                  |
| $P$         | pressure, N/m <sup>2</sup>                 |
| $P_{total}$ | total pressure, N/m <sup>2</sup>           |
| $q$         | heat flux, W/m <sup>2</sup>                |
| $R$         | bubble radius or gas constant, m or J/kg·K |
| $T$         | temperature, °C or K                       |
| $T_e$       | equilibrium temperature, °C                |
| $T_{sat}$   | saturation temperature, K                  |
| $T_w$       | surface temperature, °C                    |
| $V$         | volumetric flow rate, L/min                |
| $X$         | mole fraction in liquid, -                 |

$x$  vapor quality, -

$Y$  mole fraction in vapor, -

### Greek symbols

$\alpha$  heat transfer coefficient,  $W/m^2 \cdot K$

$\Delta T_{sub}$  degree of subcooling, K

$\xi$  ratio of heat supplied to more-volatile component to the total, -

### Subscripts

1 more-volatile component

2 less-volatile component

ave average

M midstream

out outlet

sat saturated

## Author details

Haruhiko Ohta\*, Yasuhisa Shinmoto, Daisuke Yamamoto and Keisuke Iwata

\*Address all correspondence to: [ohta@aero.kyushu-u.ac.jp](mailto:ohta@aero.kyushu-u.ac.jp)

Department of Aeronautics and Astronautics, Kyushu University, Fukuoka, Japan

## References

- [1] Vochten R. and Petre G. Study of the heat of reversible adsorption at the air-solution interface. J. Colloid Interface Sci. 2005; 42: 320-327.
- [2] Van Stralen SJD Heat transfer to boiling binary liquid mixtures at atmospheric and subatmospheric pressures. Chem. Eng. Sci. 1956; 5: 290-296.
- [3] Abe Y. Thermal management with phase change of self-wetting fluids. Proc. IM-ECE2005. 2005.
- [4] Sakai T., Yoshii S., Kajimoto K, Kobayashi H., Shinmoto Y. and Ohta H. Heat transfer enhancement observed in nucleate boiling of alcohol aqueous solutions at very low concentration. Proc. 14th Int. Heat Transfer Conf. 2010; IHTC14-22737.

- [5] Ohta H., Shinmoto Y., Ishikawa Y. and Ariki K. High Heat Flux Cooling of large areas by improved liquid supply for flow boiling in narrow channels. Proc. 13th Int. Heat Transfer Conf. (IHTC-13). 2006; CD-ROM 12 pages.
- [6] Miura S., Inada Y., Shinmoto Y. and Ohta H. Development of cooling system for a large area at high heat flux by using flow boiling in narrow channels. Proc. ASME 7th International Conference on Nanochannels, Microchannels and Minichannels (ICNMM2009). 2009; CD-ROM 8 pages.
- [7] Kobayashi H., Ohtani N. and Ohta H. Boiling heat transfer characteristics of immiscible liquid mixtures. Proc. 9th Int. Conf. on Heat Transfer, Fluid Mechanics and Thermodynamics, HEFAT2012. 2012; 771-776.
- [8] Ohnishi S., Ohta H., Ohtani N., Fukuyama Y. and Kobayashi H. Boiling heat transfer by nucleate boiling of immiscible liquids. *Interfac. Phen. Heat Transfer*. 2013; 1(1): 63-83.
- [9] Kita S., Ohnishi S., Fukuyama Y. and Ohta H. Improvement of Nucleate boiling heat transfer characteristics by using immiscible mixtures. Proc. 15th Int. Heat Transfer Conf., Kyoto, Japan. 2014; IHTC15-8941.
- [10] Filipczak G., Troniewski L. and Witczak S. Pool boiling of liquid-liquid multiphase systems, evaporation, condensation and heat transfer, Ed. Ahsan A., INTECH. 2011; Chap.6: 123-150.
- [11] Roesle ML and Kulacki FA An experimental study of boiling in dilute emulsions. Part A: Heat Transfer. *Int. J. Heat Mass Transfer*. 2012; 55(7-8): 2160-2165.
- [12] Bulanov NV and Gasanov BM Peculiarities of boiling of emulsions with a low-boiling disperse phase. *High Temp*. 2006; 44(2): 267-282.
- [13] Bonilla CF and Eisenbuerg AA Heat transmission to boiling binary mixtures. *Indus. Eng. Chem*. 1948; 40: 1113-1122.
- [14] Bragg JR and Westwater JW Film boiling of immiscible liquid mixture on a horizontal plate. *Heat Transfer* 1970. Proc. 4th Int. Heat Trans. Conf. 1970; 6: B7.1.
- [15] Sump GD and Westwater JW Boiling heat transfer from a tube to immiscible liquid-liquid mixtures. *Int. J. Heat Mass Transfer*. 1971; 14: 767-779.
- [16] Gorenflo D., Gremer F., Danger E. and Luke A. Pool boiling heat transfer to binary mixtures with miscibility gap: experimental results for a horizontal copper tube with 4.35 mm O.D. *Experiment. Thermal. Fluid Sci*. 2001; 25(5): 243-254.
- [17] Prigogine I. and Defay R. *Chemical thermodynamics*. Longmans Green and Co. 1954.
- [18] Ivey H. J. and Morris D. J. Critical heat flux of saturation and subcooled pool boiling in water at atmospheric pressure. Proc. Third Int. Heat Transfer Conf. 1966; 3: 129-142.

- [19] Green G A, Chen JC and Conlin MT Onset of entrainment between immiscible liquid layers due to rising gas bubbles. *Int. J. Heat Mass Transfer*. 1988; 31(6): 1309-1317.
- [20] Onishi S., Ohtani N., Kanazawa S. and Ohta H. Improvement nucleate boiling heat transfer characteristics by using immiscible mixtures. *Proc. 8th World Conf. Experiment. Heat Transfer Fluid Mechanics Thermodynamics (ExHFT-8)*. 2013; UFD 6 pages.
- [21] Yamasaki Y., Kita S., Iwata K., Shinmoto Y. and Ohta H. Heat transfer in boiling of immiscible mixtures. *Interfac. Pheno. Heat Transfer*. 2015; 3(1): 19-39.



